MEKONG UNIVERSITY SCIENTIFIC JOURNAL
https://tapchikhdhcl.edu.vn
https://vjol.info.vn/index.php/dhcl

FREE VIBRATION ANALYSIS OF FUNCTIONALLY GRADED SANDWICH PLATES USING A C^1-CONTINUOUS FINITE ELEMENT METHOD

Pham Quoc Hoa*, Dao Ngoc Diep
Mekong University
**Email: phamquochoa@mku.edu.vn*

Date of submission: 19/11/2025; Review Day: 28/11/2025; Date of article approval 15/12/2025

ABSTRACT

This paper proposes a finite element method utilizing a four-node quadrilateral plate element with seven degrees of freedom per node for the free vibration analysis of sandwich plates featuring a metallic core. The top and bottom face sheets are composed of ceramic-metal functionally graded materials (FGMs) whose properties vary continuously through the thickness. To accurately represent the stress - strain behavior - particularly for thick plates - Shi's third-order shear deformation theory with C^1-continuous derivatives is employed. The accuracy and convergence of the proposed formulation are verified through comparisons with benchmark results available in the literature. The novelty of this research lies in the first-time development and application of a finite element model combining Lagrange and Hermite interpolation functions to analyze the free vibration characteristics of sandwich plates.

Keywords: *sandwich plates; functionally graded material (FGM); four-node element; third-order shear deformation theory (TSDT) of Shi.*

1. Introduction

Functionally graded materials (FGMs) are advanced materials whose mechanical properties vary continuously through the thickness of the plate. They have been widely used in various scientific, engineering, and high-technology industries such as aerospace engineering, civil engineering, and nuclear power plants. The study of the behavior of structures made of FGM has attracted the attention of many researchers worldwide. Representative works include those by Hosseini-Hashemi et al. [1], who employed the first-order shear deformation theory to analyze the free vibration of FGM plates, and Reddy [2, 3], who used the higher-order shear deformation theory to investigate both linear and nonlinear behaviors of FGM plates.

A sandwich structure typically consists of two thin outer face sheets, often made of functionally graded materials (FGMs), and a thick, lightweight core made of metallic materials. This configuration provides excellent resistance to wear and bending stiffness while maintaining a low overall weight. In addition, the soft and light metallic core offers good sound and thermal insulation capabilities. Due to these superior characteristics, sandwich structures have been widely used in various high-technology and industrial fields such as aerospace engineering, aeronautics, submarine and marine engineering, and military industries. Consequently, the analysis and optimization

of such structures have attracted considerable research interest in recent years. Zarga et al. [4] employed a three-dimensional asymptotic approach to investigate the static bending behavior of sandwich plates under thermal environments. Zenkour [5] developed a four-variable shear deformation theory for the static bending analysis of sandwich plates. Natarajan et al. [6] studied both the static bending and free vibration behaviors of sandwich plates using the three-dimensional asymptotic method.

The finite element method has become a widely used tool in mechanical analysis [7]. In particular, the classical four-node rectangular element is very popular due to its simplicity and ease of computer implementation. However, using only Lagrange interpolation functions does not satisfy the C1 continuity requirement of the displacement field. Moreover, this approach fails to ensure the zero transverse shear stress condition at the top and bottom surfaces of the plate. To overcome these limitations, a four-node element with seven degrees of freedom per node is proposed in this study. The element is formulated by combining Lagrange and Hermite interpolation functions, which allows accurate determination of stresses at the top and bottom surfaces of the plate without the need for any shear locking treatment when the plate becomes thinner.

Through a review of the published studies, the authors found that no previous research has employed a four-node quadrilateral element combining Lagrange and Hermite interpolation functions for the analysis of sandwich plates. The main objective of this study is to develop a finite element method based on a newly proposed four-node element to analyze the free vibration behavior of sandwich plates. The results obtained from this study are compared with those reported in well-established references to verify the accuracy and reliability of the proposed element.

2. Theoretical Framework

2.1. Model of a Functionally Graded Sandwich Plate

A three-layer sandwich plate of dimensions *a x b* and total thickness *h* is considered (Figure 1). The bottom layer (FGM-1) and top layer (FGM-2) consist of two distinct ceramic–metal FGMs, while the core is isotropic metallic. Their respective thicknesses are h_1, h_c, and h_2.

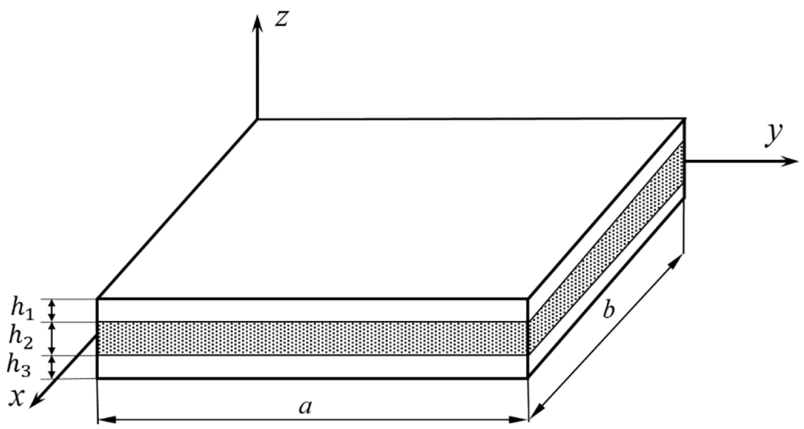

Figure 1. Model of the sandwich plate

Material properties follow the rule of mixtures [8]:

$$P(z) = P_c V_c(z) + P_m [1 - V_c(z)], \quad (1)$$

where (P_c) and (P_m) denote ceramic and metal properties, respectively. The ceramic volume fraction is given by:

$$V_c(z) = \begin{cases} \left(\frac{z+h/2}{h_1}\right)^{n_1}, & z \in [-h/2, -h/2 + h_1], \\ 1, & z \in [-h/2 + h_1, h/2 - h_2], \\ \left(\frac{h/2-z}{h_2}\right)^{n_2}, & z \in [h/2 - h_2, h/2]. \end{cases} \quad (2)$$

Table 1 shows the layer configuration, while Table 2 lists constituent material properties.

Table 1. Structure of the sandwich plateBottom layer (FGM-1)	Core layer	Top layer (FGM-2)
Al/Al2O3	Al2O3	Al2O3/Al

Table 2. Material properties used

Material constituent	Elastic modulus (GPa)	Density (kg/m³)	Poisson's ratio
Al_2O_3	380	3800	0.3
Al	70	2707	0.3

2.2. Shi's higher-order theory

Displacement field of the plate based on Shi's theory :

$$\begin{cases} u(x,y,z) = u_0(x,y) + \frac{5}{4}\left(z - \frac{4}{3h^2}z^3\right)\varphi_x(x,y) + \left(\frac{1}{4}z - \frac{5}{3h^2}z^3\right)w_{0,x} \\ v(x,y,z) = v_0(x,y) + \frac{5}{4}\left(z - \frac{4}{3h^2}z^3\right)\varphi_y(x,y) + \left(\frac{1}{4}z - \frac{5}{3h^2}z^3\right)w_{0,y} \\ w(x,y,z) = w_0(x,y) \end{cases} \quad (3)$$

where u_0, v_0, w_0, φ_x and φ_y are the displacement parameters of the plate. In particular, u_0, v_0, w_0 represent the displacements of the mid-surface in the x, y, and z directions, respectively, while φ_x, φ_y denote the rotations of the normal about the y– and x–axes, respectively.

The strain field can be derived from the displacement field as follows:

$$\boldsymbol{\varepsilon} = \boldsymbol{\varepsilon}_m + z\boldsymbol{\kappa}_1 + z^3\boldsymbol{\kappa}_2 \quad (4)$$

here

Membrane strains $\boldsymbol{\varepsilon}_m$:

$$\boldsymbol{\varepsilon}_m = \begin{Bmatrix} u_{0,x} \\ v_{0,y} \\ u_{0,y} + v_{0,x} \end{Bmatrix} \quad (5)$$

Bending strains $\boldsymbol{\kappa}_1$, $\boldsymbol{\kappa}_2$:

$$\boldsymbol{\kappa}_1 = \frac{1}{4}\begin{Bmatrix} 5\varphi_{x,x} + w_{,xx} \\ 5\varphi_{y,y} + w_{,yy} \\ 5\varphi_{x,y} + 2w_{,xy} + 5\varphi_{y,x} \end{Bmatrix} \quad (6)$$

$$\boldsymbol{\kappa}_2 = \frac{-5}{3h^2}\begin{Bmatrix} \varphi_{x,x} + w_{,xx} \\ \varphi_{y,y} + w_{,yy} \\ \varphi_{x,y} + 2w_{,xy} + \varphi_{y,x} \end{Bmatrix} \tag{7}$$

Shear strain $\boldsymbol{\gamma}$ is:

$$\boldsymbol{\gamma} = \boldsymbol{\gamma}_0 + z^2\boldsymbol{\gamma}_1 \tag{8}$$

in which

$$\boldsymbol{\gamma}_0 = \frac{5}{4}\begin{Bmatrix} w_{,y} + \varphi_y \\ w_{,x} + \varphi_x \end{Bmatrix}; \boldsymbol{\gamma}_1 = \frac{-5}{h^2}\begin{Bmatrix} w_{,y} + \varphi_y \\ w_{,x} + \varphi_x \end{Bmatrix} \tag{9}$$

The relationship between stress and strain according to Hooke's law is as follows:

$$[\mathbf{N} \quad \mathbf{M} \quad \mathbf{P}]^T = \mathbf{D}_m[\boldsymbol{\varepsilon}_m \quad \boldsymbol{\kappa}_1 \quad \boldsymbol{\kappa}_2]^T; \ [\mathbf{Q} \quad \mathbf{R}]^T = \mathbf{D}_s[\boldsymbol{\gamma}_0 \quad \boldsymbol{\gamma}_1]^T \tag{10}$$

here

$$\mathbf{D}_m = \begin{bmatrix} \mathbb{A} & \mathbb{B} & \mathbb{B}^b \\ \mathbb{B} & \mathbb{F} & \mathbb{F}^b \\ \mathbb{B}^b & \mathbb{F}^b & \mathbb{H} \end{bmatrix}; \mathbf{D}_s = \begin{bmatrix} \mathbb{A}^s & \mathbb{B}^s \\ \mathbb{B}^s & \mathbb{F}^s \end{bmatrix} \tag{11}$$

in which

$$(\mathbb{A}, \mathbb{B}, \mathbb{B}^b, \mathbb{F}, \mathbb{F}^b, \mathbb{H}) = \int_{\frac{-h}{2}}^{\frac{h}{2}} \frac{E(z)}{1-\nu(z)^2}\begin{bmatrix} 1 & \nu(z) & 0 \\ \nu(z) & 1 & 0 \\ 0 & 0 & \dfrac{1}{2(1-\nu(z))} \end{bmatrix}(1, z, z^2, z^3, z^4, z^6)\mathrm{d}z \tag{12}$$

and

$$(\mathbb{A}^s, \mathbb{B}^s, \mathbb{F}^s) = \int_{\frac{-h}{2}}^{\frac{h}{2}} \frac{E(z)}{2(1+\nu(z))}\begin{bmatrix} 1 & 0 \\ 0 & 1 \end{bmatrix}(1, z^2, z^4)\mathrm{d}z \tag{13}$$

Equation (10) can be expressed in matrix form as follows:

$$\begin{bmatrix} \mathbf{N} \\ \mathbf{M} \\ \mathbf{P} \\ \mathbf{Q} \\ \mathbf{R} \end{bmatrix} = \begin{bmatrix} \mathbb{A} & \mathbb{B} & \mathbb{B}^b & 0 & 0 \\ \mathbb{B} & \mathbb{F} & \mathbb{F}^b & 0 & 0 \\ \mathbb{B}^b & \mathbb{F}^b & \mathbb{H} & 0 & 0 \\ 0 & 0 & 0 & \mathbb{A}^s & \mathbb{B}^s \\ 0 & 0 & 0 & \mathbb{B}^s & \mathbb{F}^s \end{bmatrix}\begin{bmatrix} \boldsymbol{\varepsilon}_m \\ \boldsymbol{\kappa}_1 \\ \boldsymbol{\kappa}_2 \\ \boldsymbol{\gamma}_0 \\ \boldsymbol{\gamma}_1 \end{bmatrix} \tag{14}$$

2.3. Governing Differential Equation of the Sandwich Plate

Based on [10], the differential equation is:

$$\mathbf{L}(\mathbf{u}) + \rho h\ddot{\mathbf{u}} = 0, \tag{15}$$

with strain energy:

$$U = \frac{1}{2}\int_V \boldsymbol{\varepsilon}^T \boldsymbol{\sigma}\, dV, \tag{16}$$

and kinetic energy defined by (17)–(20). The weak form is:

$$\delta U - \delta T = 0. \tag{21}$$

2.4. Finite Element Method

The nodal displacement vector of the quadrilateral element is expressed as follows (see Figure 2):

$$\boldsymbol{q}_e = [\boldsymbol{q}_1^T \quad \boldsymbol{q}_2^T \quad \boldsymbol{q}_3^T \quad \boldsymbol{q}_4^T]^T \tag{22}$$

$\boldsymbol{q}_i$ $(i = 1 \div 4)$ is described as follows:

$$\boldsymbol{q}_i = \{u_{0i} \quad v_{0i} \quad w_i \quad \varphi_{xi} \quad \varphi_{yi} \quad \theta_{xi} = w_{i,x} \quad \theta_{yi} = w_{i,y}\} \tag{23}$$

here

u_0, v_0, φ_x and φ_y interpolated using Lagrange shape functions (see Appendix):

$$\{u_0 \quad v_0 \quad \varphi_x \quad \varphi_y\} = \left[\sum_{i=1}^4 N_i u_{0i} \ldots \quad \sum_{i=1}^4 N_i v_{0i} \ldots \quad \sum_{i=1}^4 N_i \varphi_{xi} \ldots \quad \sum_{i=1}^4 N_i \varphi_{yi} \ldots\right]^T; \tag{24}$$

$$w = H_1 w_1 + H_2 w_{1,x} + H_3 w_{1,y+\cdots+} H_{10} w_4 + H_{11} w_{4,x} + H_{12} w_{4,y} \tag{25}$$

$$\begin{aligned} \theta_x &= w_{,x} + \varphi_x \\ &= \frac{\partial}{\partial x}\left(H_1 w_1 + H_2 w_{1,x} + H_3 w_{1,y+\cdots+} H_{10} w_4 + H_{11} w_{4,x} + H_{12} w_{4,y}\right) \\ &+ \sum_{i=1}^4 N_i \varphi_{xi} \end{aligned} \tag{26}$$

$$\begin{aligned} \theta_y &= w_{,y} + \varphi_y \\ &= \frac{\partial}{\partial y}\left(H_1 w_1 + H_2 w_{1,x} + H_3 w_{1,y+\cdots+} H_{10} w_4 + H_{11} w_{4,x} + H_{12} w_{4,y}\right) \\ &+ \sum_{i=1}^4 N_i \varphi_{yi} \end{aligned} \tag{27}$$

To satisfy the stress-free conditions on the top and bottom surfaces of the plate, the derivatives of w in the x- and y-directions are assumed as two degrees of freedom θ_x and θ_y, and are approximated using Hermite functions as follows (see Appendix):

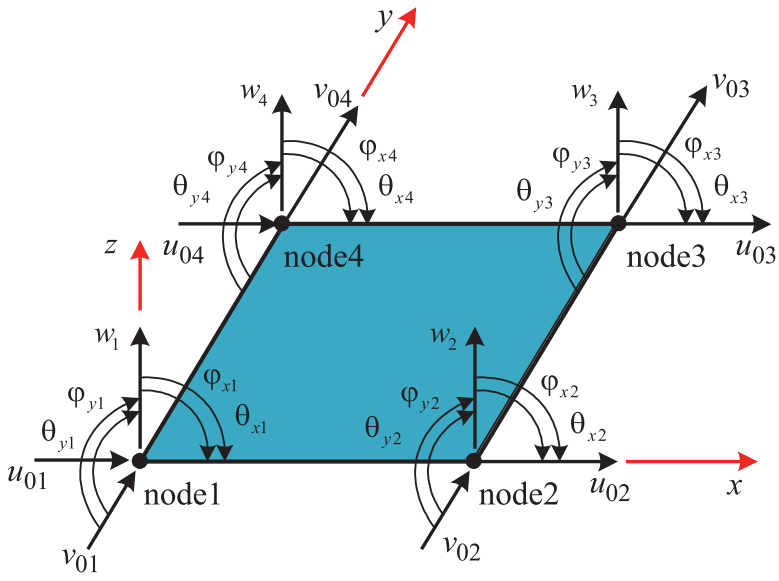

Figure 2. Four-node quadrilateral element model with seven degrees of freedom per node.

Substituting Equations (25), (26), and (27) into Equations (5), (6), (7), and (8), the strain field vectors can be expressed as follows:

$$\boldsymbol{\varepsilon} = [\mathbf{B}_1 \quad \mathbf{B}_2 \quad \mathbf{B}_3]\boldsymbol{q}_e; \tag{28}$$

$$\boldsymbol{\gamma} = [\mathbf{B}_4 \quad \mathbf{B}_5]\boldsymbol{q}_e \tag{29}$$

By substituting Equations (28) and (29) into Equation (23), the governing equation of the plate can be rewritten as follows:

$$\boldsymbol{M}_e\ddot{\boldsymbol{q}}_e + \boldsymbol{K}_e\boldsymbol{q}_e = \mathbf{0} \tag{30}$$

in which

The stiffness matrix $\boldsymbol{K}_e$ is:

$$\boldsymbol{K}_e = \int_S \left(\begin{Bmatrix} \boldsymbol{B}_1 \\ \boldsymbol{B}_2 \\ \boldsymbol{B}_3 \\ \boldsymbol{B}_4 \\ \boldsymbol{B}_5 \end{Bmatrix}^T \begin{bmatrix} \mathbb{A} & \mathbb{B} & \mathbb{B}^b & 0 \\ \mathbb{B} & \mathbb{F} & \mathbb{F}^b & 0 \\ \mathbb{B}^b & \mathbb{F}^b & \mathbb{H} & 0 \\ 0 & 0 & \mathbb{A}^s & \mathbb{B}^s \\ 0 & 0 & \mathbb{B}^s & \mathbb{F}^s \end{bmatrix} \begin{Bmatrix} \boldsymbol{B}_1 \\ \boldsymbol{B}_2 \\ \boldsymbol{B}_3 \\ \boldsymbol{B}_4 \\ \boldsymbol{B}_5 \end{Bmatrix} \right) \mathrm{dS} \tag{31}$$

here $\boldsymbol{N}$ is the shape function matrix of the element:

$$\boldsymbol{N} = \sum_{i=1}^{4} \begin{bmatrix} N_i & 0 & 0 & 0 & 0 & 0 & 0 \\ 0 & N_i & 0 & 0 & 0 & 0 & 0 \\ 0 & 0 & H_{(3i-2)} & 0 & 0 & H_{(3i-1)} & H_{3i} \\ 0 & 0 & 0 & N_i & 0 & 0 & 0 \\ 0 & 0 & 0 & 0 & N_i & 0 & 0 \\ 0 & 0 & \frac{\partial}{\partial\zeta}H_{(3i-2)} & 0 & 0 & \frac{\partial}{\partial\zeta}H_{(3i-1)} & \frac{\partial}{\partial\zeta}H_{3i} \\ 0 & 0 & \frac{\partial}{\partial\chi}H_{(3i-2)} & 0 & 0 & \frac{\partial}{\partial\chi}H_{(3i-1)} & \frac{\partial}{\partial\chi}H_{3i} \end{bmatrix} \tag{33}$$

The governing differential equation of the plate expressed in matrix form is as follows:

$$\boldsymbol{M}\ddot{\boldsymbol{q}} + \boldsymbol{K}\boldsymbol{q} = \mathbf{0} \leftrightarrow |\boldsymbol{K} - \omega^2\boldsymbol{M}| = \mathbf{0} \tag{34}$$

here ω is the natural frequency of the plate structure; $\boldsymbol{K} = \sum_{nel}\boldsymbol{K}_e$, $\boldsymbol{M} = \sum_{nel}\boldsymbol{M}_e$ are the global stiffness matrix and the global mass matrix.

3. Numerical results

In this section, the authors compute the natural frequencies of the sandwich plate and compare them with previously published studies to confirm the accuracy and efficiency of the computational method proposed in this paper. The finite element method is employed using different mesh sizes. Table 3 presents the first frequency of the Al/Al_2O_3 functionally graded sandwich plate, defined as $\omega^* = \omega \frac{a^2}{h}\sqrt{\frac{\rho_0}{E_0}}$ **với** $(\rho_0 = 1kg/m^3, E_0 = 1GPa)$. The results obtained using the present element with a 16×16 mesh are very close to those reported by Li et al. [11] and Bessaim et al. [12]**.** Based on these comparisons, the authors conclude that the 16×16 mesh is appropriate for analyzing sandwich plate structures.

In addition, the table shows that as k_1, k_2 increase, the plate's natural frequency also increases. This can be explained by the increase in the ceramic fraction on the top and bottom surfaces, which makes the plate stiffer and thus leads to higher frequencies. Moreover, the results indicate that the 1-1-1 sandwich configuration always yields the highest natural frequency, while the other two configurations result in lower frequencies. These findings allow engineers to select the most suitable sandwich configuration for practical engineering applications. Figure 3 provides a visual display of the vibration modes of the sandwich plate, helping readers better understand the vibration behavior of such plates in engineering practice.

Table 3. First normalized frequencies

Figure 3 illustrates the first six mode shapes, offering insight into vibration behavior.

k_1=k_2	Mesh size	Sandwich configuration								
		1-1-1			2-2-1			1-2-1		
		Proposed method	[11]	[12]	Proposed method	[11]	[12]	Proposed method	[11]	[12]
0	(10x10)	0.93022	0.92897	0.92897	0.93022	0.92897	0.92897	0.93022	0.92897	0.92897
	(12x12)	0.92946			0.92946			0.92946		
	(14x14)	0.92901			0.92901			0.92901		
	(16x16)	0.92872			0.92872			0.92872		
	(18x18)	0.92872			0.92872			0.92872		
0.5	(10x10)	1.48947	1.48459	1.48853	1.43901	1.43419	1.4404	1.41791	1.41662	1.41788
	(12x12)	1.48859			1.43818			1.41714		
	(14x14)	1.48806			1.43769			1.41668		
	(16x16)	1.48772			1.43736			1.41638		
	(18x18)	1.48772			1.43736			1.41638		

1	(10x10)	1.64301	1.63053	1.64199	1.58226	1.57037	1.5843	1.56247	1.55788	1.56301
	(12x12)	1.64202			1.58136			1.56165		
	(14x14)	1.64143			1.58081			1.56116		
	(16x16)	1.64105			1.58046			1.56085		
	(18x18)	1.64105			1.58046			1.56085		
5	(10x10)	1.82199	1.78956	1.82032	1.75968	1.72726	1.75972	1.74793	1.7267	1.75143
	(12x12)	1.82071			1.75852			1.74689		
	(14x14)	1.81993			1.75783			1.74627		
	(16x16)	1.81943			1.75738			1.74587		
	(18x18)	1.81943			1.75738			1.74587		
10	(10x10)	1.84213	1.80813	1.83973	1.78527	1.74779	1.78163	1.77359	1.74811	1.77878
	(12x12)	1.84078			1.78405			1.77248		
	(14x14)	1.83997			1.78332			1.77182		
	(16x16)	1.83944			1.78284			1.77139		
	(18x18)	1.83944			1.78284			1.77139		

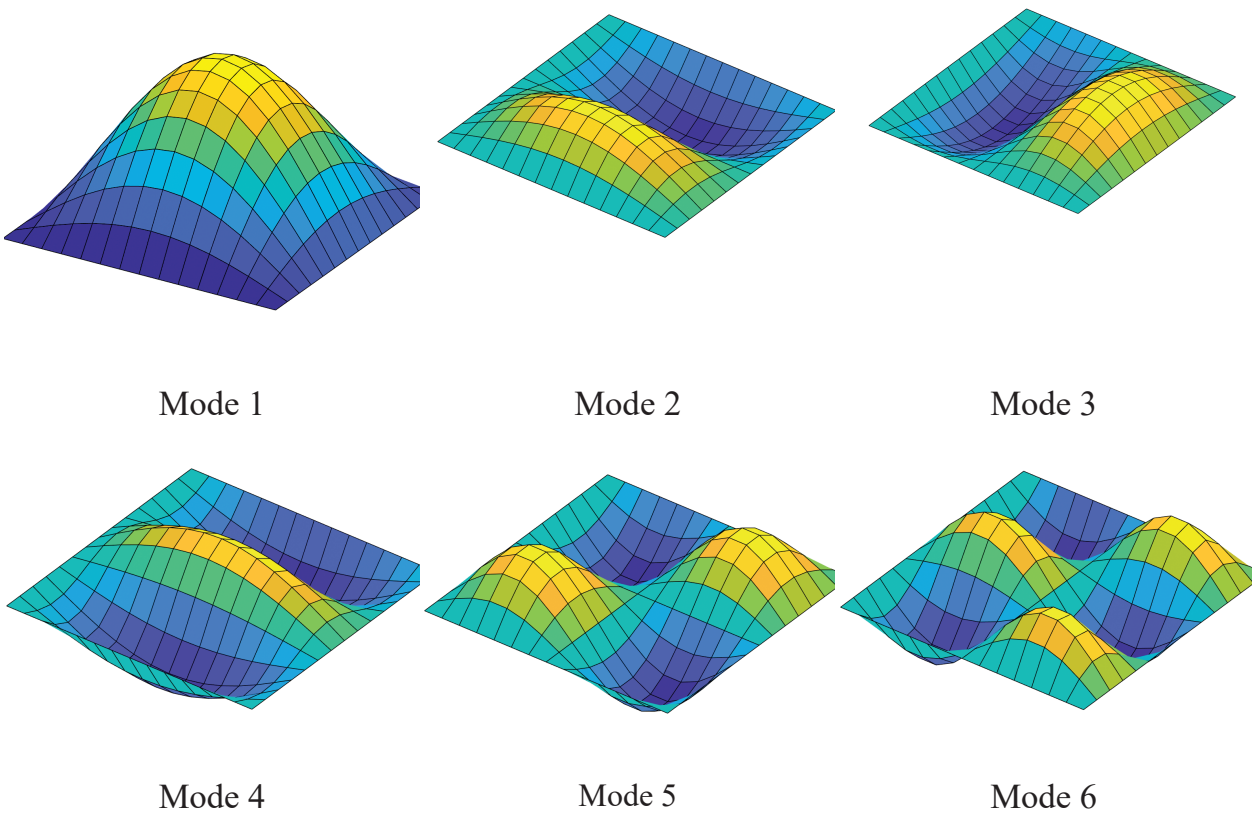

Figure 3. Vibration modes of the sandwich plate

4. Conclusion

This paper presents a new C^1-continuous finite element formulation for free vibration analysis of functionally graded sandwich plates. The proposed four-node quadrilateral element with seven degrees of freedom per node - based on combined Lagrange and Hermite interpolation - accurately captures both bending and shear behavior without shear correction. Comparisons with benchmark results confirm excellent accuracy and convergence. The method is robust, computationally efficient, and applicable to advanced structural designs in aerospace, marine, and defense engineering.

REFERENCES

Hosseini-Hashemi, S., Taher, H. R. D., Akhavan, H., Omidi, M. (2010), Free vibration of functionally graded rectangular plates using first-order shear deformation plate theory, *Applied Mathematical Modelling*, *34*(5), pp. 1276–1291.

Reddy, J. N. (2000), Analysis of functionally graded plates, *International Journal for Numerical Methods in Engineering*, *47*, pp. 663–684.

Reddy, J. N. (2011), A general nonlinear third-order theory of functionally graded plates, *International Journal of Aerospace and Lightweight Structures*, *1*, pp. 1–21.

Zarga, D., Tounsi, A., Bousahla, A. A., Bourada, F., Mahmoud, S. R. (2019), Thermomechanical bending study for functionally graded sandwich plates using a simple quasi-3D shear deformation theory, *Steel and Composite Structures*, *32*(3), pp. 389–410.

Zenkour, A. M. (2013), Bending analysis of functionally graded sandwich plates using a simple four-unknown shear and normal deformations theory, *Journal of Sandwich Structures and Materials*, *15*, pp. 629–656.

Natarajan, S., Manickam, G. (2012), Bending and vibration of functionally graded material sandwich plates using an accurate theory, *Finite Elements in Analysis and Design*, *57*, pp. 32–42.

Hein, A., Vekinis, G., Kilikoglou, V. (2022), Modeling of biaxial flexure tests of transport amphorae with the finite element method: Fracture strength, deformation and stress distribution, *Results in Engineering*, *15*, p. 100508.

Alibeigloo, A., Alizadeh, M. (2015), Static and free vibration analyses of functionally graded sandwich plates using state space differential quadrature method, *European Journal of Mechanics – A/Solids*, *54*, pp. 252–266.

Shi, G. (2007), A new simple third-order shear deformation theory of plates, *International Journal of Solids and Structures*, *44*, pp. 4399–4417.

Reddy, J. N. (2003), *Mechanics of Laminated Composite Plates and Shells: Theory and Analysis*, CRC Press.

Li, Q., Iu, V. P., Kou, K. P. (2008), Three-dimensional vibration analysis of functionally graded material sandwich plates, *Journal of Sound and Vibration*, *311*, pp. 498–515.

Bessaim, A., Houari, M. S. A., Tounsi, A., Mahmoud, S. R., El Abbas, A. B. (2013), A new higher-order shear and normal deformation theory for the static and free vibration analysis of sandwich plates with functionally graded isotropic face sheets, *Journal of Sandwich Structures and Materials, 15(6),* pp. 671–703.